SIN-CHN SCIENTIFIC PRESS PTE.LTD.

Molecular & Cellular Biomechanics 2024, 21(4), 661.
https://doi.org/10.62617/mcb661

Article

Drug-carrying properties and targeted delivery of biomimetic nanoparticles delivering wild baicalin and Adriamycin

Menglu Wang[1,*], Yulin Li[2], Songwei Zhao[1]

[1] Hebi Polytechnic, Hebi 458030, China
[2] Henan Provincial Biotechnology Research Center, Zhengzhou 450000, China
*** Corresponding author:** Menglu Wang, wml202409@126.com

CITATION

Wang M, Li Y, Zhao S. Drug-carrying properties and targeted delivery of biomimetic nanoparticles delivering wild baicalin and Adriamycin. Molecular & Cellular Biomechanics. 2024; 21(4): 661. https://doi.org/10.62617/mcb661

ARTICLE INFO

Received: 30 October 2024
Accepted: 13 November 2024
Available online: 26 December 2024

Abstract: The extensive application of biomaterials and nanotechnology in biomedical technology can enhance the drug-carrying performance and targeted therapeutic ability of drug nanoparticles. In the article, biomimetic nanoparticles of wild baicalin and adriamycin were prepared based on conventional means, and the drug release performance of SCU/DOX was analysed using drug release kinetics and the inhibitory effect of SCU/DOX nanoparticles on tumour cells. The nanoparticles were produced through nanotechnology after the main experimental scheme was prepared for the preparation of the basic medicine. At the same time, the study combines the biological electrical signal to obtain the value of the relevant measurement index. When the SCU/DOX nanodrug concentration was elevated from 10 μM to 16010 μM, the viability of mouse tumour cells was reduced from 82.54% to about 47.69%. This shows that nanoparticles can effectively deliver drugs. After the use of SCU drug alone and SCU/DOX nanoparticles, the IC50 values of both were 59.42 μM and 8.75 μM, respectively, with a reversal of resistance multiplier of 6.79-fold. Tumour cell treatment with SCU/DOX nanoparticles reduced the tumour volume from 15.1*102mm^3 to 6.05*102mm^3 and tumour weight by 64.14% in mice. The cumulative drug release from SCU/DOX nanoparticles was 11.18% at 2h, and higher than that of the esterase-free condition after 20h (17.61%). The data of the cumulative release of the drug show that the release of biomimetic nanoparticles can actually target the target. The unique quality of nanomaterials can allow drugs to release drugs in the set target environment. On the basis of this study, if clinical trials can also achieve good results, they are expected to be applied in practice. The preparation of baicalin and adriamycin mimetic nanoparticles based on the drug delivery system can enhance the drug-carrying property and target delivery effect of the drug, which can provide a reliable technical support to enhance the therapeutic effect of the disease.

Keywords: wild baicalin; adriamycin; bionanoparticles; drug release kinetics; SCU/DOX; drug-loading performance

1. Introduction

With the continuous development of nanotechnology, nanomaterials have been widely used in the fields of biosensing, catalysis, and nanomedicine by virtue of their unique size and surface effects. Especially in the field of nanomedicine, nanomaterials provide a variety of platforms that can be used for tumour diagnosis and treatment [1–3]. In recent years, much of the slow release of drugs has been achieved through nanostructures. This is due to the potent pharmacological response of nanostructures to deliver drugs to the desired site, thereby reducing side effects. Therefore, nanocarriers, as an emerging platform for cancer therapy, are expected to efficiently solve the problems associated with drug delivery [4–7].

Nanoparticles refer to solid colloidal particles formed from polymers with a particle size between 10 nm and 1000 nm. Traditionally, nanoparticles are mainly prepared from polymers such as poly (ethylene glycol), poly (lactic acid), and poly(caprolactone) [8–10]. Nanodrug delivery systems use nanocarriers such as micelles, polymer nanoparticles, liposomes, etc., to incorporate drugs into nanoparticles by chemical bonding or physical embedding, which can improve drug stability, bioavailability, targeting, and reduce drug toxicity [11–14]. Compared to other dosage forms, nanoparticles have the advantages of smaller particle size, larger surface area, and greater ability to penetrate cells [15–16]. Nanoparticles can be prepared from both organic and inorganic materials, and functional inorganic nanoparticle delivery systems such as titanium dioxide nanoparticles have been widely used in biomedical applications [17–18].

Nanomaterial-based nanodrug delivery systems can achieve slow and controlled release of drugs and targeted delivery to improve the therapeutic effects of diseases. In this paper, the specific forms of nanomedicine delivery in vivo and their delivery barriers are analysed, and the kinetic models of nanomedicine release are explored from the zero-level, one-level, Higuchi model, Korsmeyer-Peppas model, Hixon-Crowell model and Baker-Lonsdale model. SCU/DOX nanoparticles of wild baicalin and adriamycin were prepared using relevant experimental materials and tested for drug analysis, cell proliferation and toxicity effects, and drug release. The inhibitory effects of SCU/DOX mimetic nanoparticles on tumour cell viability and cell proliferation were analysed in depth, and quantitative analyses were also carried out for the drug release properties and kinetics of SCU/DOX nanoparticles.

2. Theoretical foundations

Conventional means in drug formulation, such as structural modification of drugs, addition of stabilisers and absorption enhancers, are unable to simultaneously solve the problems of permeability, stability, immunogenicity and targeting during the in vivo delivery of biomolecule drugs. Thus, the establishment of biomimetic nanoparticles for drug delivery and release systems can enhance the stability of biomolecular drugs delivered in vivo, stabilise the structure of biomolecular drugs based on biomimetic nanoparticles, facilitate their penetration through biological barriers and improve their distribution in vivo, so as to better realise the targeted therapeutic properties of drugs.

2.1. Nano drug delivery systems

The degree of activity to release the payload at a specific location with controlled release at a lesser dose and toxicity is termed as smartness of the drug carrier system [19]. This activity of intelligent drug carrier systems is based on a number of factors that make it more suitable for drug delivery as compared to conventional systems. Conventional systems have limitations in terms of payload, site-specific release in response to external or internal stimuli. This can be achieved by functionalisation or targeting of conventional drug carrier systems. The characteristics of smart drug carriers are as follows:

(1) Ability to avoid blood degradation.

(2) Site-specific release with controlled rates and concentrations.

(3) Stimulation of response.

(4) Co-delivery of nucleic acids, proteins, etc.

Functionalisation of traditional drug delivery systems offers great opportunities for drug delivery, and the number of proteins expressed by diseased cells like anticancer cells can be used as markers to differentiate between normal and cancerous cells. Vascular endothelial growth factor (VEGF), a mediator of neovascularisation, is over-regulated in cancer cells and signals using matching ligands can control these cells. Drug release from the matrix at a controlled rate is a key factor in drug release and can be addressed by the delivery system in response to internal or external stimuli or by decorating the surface with various chemical groups.

Depending on the size, material and shape, various structures of nanoparticles for drug delivery can be designed. Each particle is different in terms of potential drug loading, drug immobilisation particles, drug release rate and targeted delivery efficiency. The classes of nanodrug carriers are shown in **Figure 1** and the common ones are dendrimers, micelles, polymeric nanoparticles, hydrogels, liposomes and vesicles.

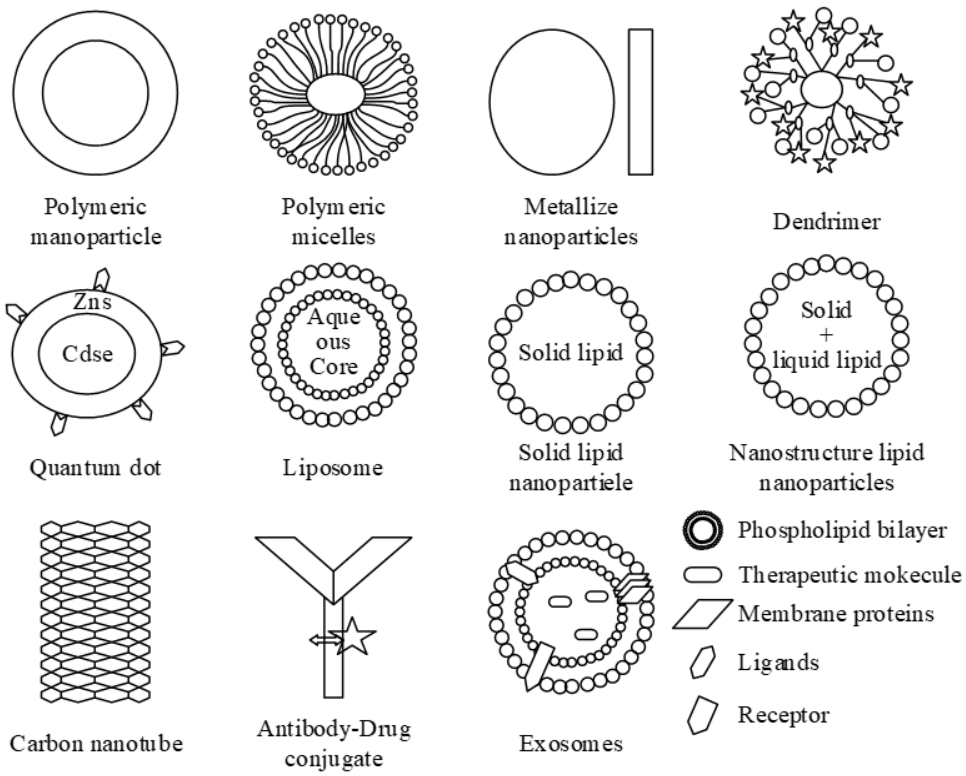

Figure 1. Category of nanodrug carriers.

2.2. Nanomedicine in vivo delivery and barriers

In the vast majority of cases, the site of action of chemotherapeutic drugs is located in subcellular structures such as DNA or mitochondria within the tumour cell (the same is true for therapeutic materials used in radiotherapy, photodynamic and photothermal therapy), so the journey of nanomedicines from injection into the body

to their functioning can be summarised in the following five stages, i.e., in vivo circulation, tumour enrichment, tumour infiltration, entry into the cell and drug release [20]. Each stage is in a different physiological environment, and the physiological barriers that the nanomedicine needs to overcome are also different, and the characteristics of the nanomedicine need to be different, as follows:

(1) In vivo circulation. After entering the body, the nanomedicine should firstly enter the circulatory system, which can ensure that the nanomedicine has a longer blood circulation time (i.e., long circulation) in the body, which is the premise that the nanomedicine can be effectively enriched in the tumour.

(2) Tumour enrichment. Due to the toxic side effects of anti-tumour drugs, enabling anti-tumour drugs to be enriched within tumours is a necessary element for current highly effective chemotherapeutic drugs. We attribute the enrichment of nanomedicines in tumours to four pathways, i.e., passive targeting, active targeting I, active targeting II, and active targeting III.

(3) Tumour penetration. Nanomedicines are able to increase the drug concentration within the tumour without increasing the toxic side effects, i.e., achieving drug enrichment within the tumour. However, the enrichment of nano-drugs in the tumour is only limited to the vicinity of the tumour blood vessels, so that the tumour cells near the blood vessels are under higher drug concentration, however, the drug concentration in the depth of the tumour is almost zero, which does not play a therapeutic effect.

(4) Entering cells. Chemotherapeutic drugs need to enter the cells to play a role, usually the pathway of chemotherapeutic drugs into the cells can be divided into two, one is that the nanomedicine releases the drug outside the tumour cells, and the free drug enters into the cells, and the other is that the nanomedicine enters into the tumour cells, and then releases the drug.

(5) Drug release. Usually, the therapeutic activity of the drug can only be activated by releasing it from its carrier, and the enrichment of the nanocarrier alone cannot enhance the concentration of the effective drug, so the design demand of this process requires that the nanocarrier can rapidly release the encapsulated drug at the cancer site.

2.3. Nano-drug release kinetics

The mechanism of drug release is closely related to the type of material and can be fitted and analysed by several models, i.e., zero-stage release kinetic model, one-stage kinetic model, Higuchi's equation, Peppas' model, Gallagher-Corrigan model, Weibull's distribution, etc. [21]. Some of the mathematical models of drug release kinetics are as follows:

(1) Zero-stage release kinetics

Zero-stage release kinetic model, i.e., the rate of drug release is constant and independent of time and drug concentration factors. Then:

$$M_t / M_\infty = kt \tag{1}$$

where, M_t / M_∞ is the cumulative release rate of the drug at t time, k is the kinetic release rate constant for zero level release and t is the release time. The release curve

was plotted and linearly fitted with release time t as the horizontal coordinate and cumulative release rate M_t/M_∞ as the vertical coordinate.

(2) First order kinetic model, i.e., the rate of drug release is proportional to the drug in the extended-release formulation. Namely:

$$M_t/M_\infty = 1-e^{-kt} \tag{2}$$

where M_t/M_∞ is the cumulative release rate of the drug at t time, k is the number of release kinetics at the first level, and t is the release time. The equation can be reduced to logarithmic form by transformation, i.e.:

$$ln\left(1-\frac{M_t}{M_\infty}\right) = -kt \tag{3}$$

A linear fit was performed with release time t as the horizontal coordinate and $ln\left(1-\frac{M_t}{M_\infty}\right)$ as the vertical coordinate.

(3) Higuchi model

In Higuchi model, the cumulative rate of drug release is proportional to the square root of time with the following equation:

$$M_t/M_\infty = kt^{1/2} \tag{4}$$

where, M_t/M_∞ is the cumulative release rate of the drug at t time, k is the release rate constant and t is the release time. According to the release results, the release time t is the horizontal coordinate and the cumulative release rate M_t/M_∞ is the vertical coordinate.

(4) Korsmeyer-Peppas model, which is expressed as follows:

$$M_t/M_\infty = kt^n \tag{5}$$

where, M_t/M_∞ is the cumulative release rate of the drug at t time, k is the release rate constant, t is the release time and n is the diffusion index. The release mechanism of this release model is able to be judged by the n value. According to the different types of materials are classified into soluble and insoluble systems. For the soluble spherical material, the release mechanism is Fick diffusion when $n=0.43$, anomalous diffusion when $0.43<n<0.85$, and CaseII release when $n=0.85$. For insoluble spherical materials, when $n=0.43$, the release mechanism is also Fick diffusion, when $0.43<n<1.0$, the release mechanism is anomalous diffusion, and when $n=1.0$, the release mechanism is Case I release.

(5) The Hixon-Crowell model, which can be expressed as:

$$W_0^{1/3} - W_t^{1/3} = K_c t \tag{6}$$

where W_0 is the initial drug dose, W_t is the remaining drug dose of the drug at moment t, and K_c is the Hixon-Crowell dissolution rate constant. This model assumes that the release rate is limited by the drug's novel dissolution rate and is not affected by diffusion.

(6) Baker-Lonsdale model which can be expressed as:

$$F_t = \frac{3}{2} \times \left[1 - \left(1 - \frac{M_t}{M_\infty}\right)^{\frac{2}{3}}\right] - \frac{M_t}{M_\infty} = K_B t \tag{7}$$

where K_B is the kinetic constant of drug release.

3. Materials and methods

In order to achieve higher disease therapeutic effects and lower toxicity, evolving drug delivery technologies provide new ideas for drug carriers and targeted therapies. Delivery systems are designed according to the nature of the drug itself to improve the solubility of the drug, to achieve a slow release of the drug, and to increase the bioavailability. By improving the prescription and process of nanoparticles in order to adjust their surface properties, or modifying specific targeting molecules, precise modulation and treatment of the corresponding targets can be achieved. This chapter focuses on biomimetic nanoparticles prepared by fusion of wild baicalin (SCU) and adriamycin (DOX) as a way to enhance their drug-carrying properties and targeted therapeutic capabilities.

3.1. SCU pharmacological effects

Wild baicalin is a flavonoid extracted from Lampsia officinalis with the molecular formula C21H18O12, and its chemical structure is shown in **Figure 2**. Studies have shown that SCU possesses a range of pharmacological activities, such as antioxidant, anti-inflammatory, and neuroprotective [22]. SCU has effective anticancer effects against many types of tumours, including hepatocellular carcinoma, colorectal carcinoma, and squamous carcinoma of the tongue. Moreover, SCU has low toxicity and few reports on toxicology. This property of good efficacy and low toxicity makes wild scutellarin have a good prospect for development and application.

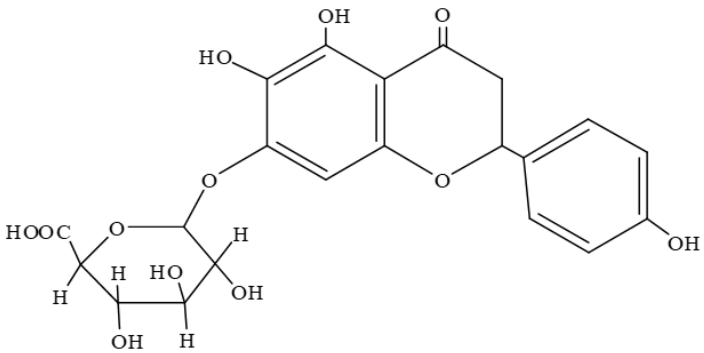

Figure 2. Structural formula of SCU.

(1) Anti-tumour effects: SCU has the ability to inhibit the proliferation of non-small cell lung cancer (NSCLC) cells, PC-9 and H1975, promote apoptosis and induce autophagy. The mechanism of action analysis revealed that SCU-induced autophagy was closely related to the activation of ERK1/2 signalling pathway and the inhibition of AKT pathway.

(2) Antioxidant effect: SCU has a significant scavenging effect on hydroxyl radicals (-OH), superoxide anion radicals (O2-) and hydrogen peroxide, and it can protect ARPE-19 cells from H_2O_2-induced oxidative damage through activation of the JAK2/STAT3 signalling pathway.

(3) Anti-inflammatory effect: SCU has a good anti-inflammatory effect and can inhibit the expression of inflammatory factors IL-1β, IL-6 and TNF-α. Oral administration of SCU can significantly inhibit the inflammatory response and cartilage degeneration in arthritis models. Its anti-inflammatory mechanism was related to NFκB and PI3K/AKT signalling pathways.

(4) Neuroprotective effect. SCU has a protective effect against neuronal injury, can alleviate the damage of neuronal cells, reduce brain water content, regulate the expression of glutamate (Glu), aspartic acid (Asp), glycine (Gly), γ-aminobutyric acid (GABA) and taurine (Tau), and improve the activities of Ca^{2+}-ATPase and Na^+ and K^+-ATPase.

(5) Bone differentiation promotion: SCU dose-dependently enhances cell proliferation, alkaline phosphatase (ALP) activity, and calcium deposition in human osteoblasts by increasing the levels of CXCR4 mRNA and protein expression, as well as osteoblast anabolism.

3.2. Preparation of experimental materials

3.2.1. Experimental reagents and consumables

The experimental animals selected for this paper were 30 healthy SPF-grade male C57BL/8 mice, 8–12 weeks, weighing 24 g–28 g, purchased from a laboratory animal technology company. All animal experiments were approved by the Medical Ethics Committee of Q University Hospital.

The main reagents and consumables were as follows:

Wild baicalin was purchased from MCE (CAS-27740-01, purity > 98.5%, catalogue number HY-N0748). Wild baicalin was dissolved in DMSO and then diluted to a final concentration of 8.5 g/L (18.05 mmol/L) using 0.85% NaCl solution and filtered using a 0.15 μm filter membrane. The final concentration of DMSO was 0.56% in all solutions added to the cells in this study.

RPMI-1640 medium was purchased from H USA. Fetal bovine serum (FBS), trypsin (0.26%), 1.2% penicillin, and streptomycin were purchased from G, USA. Phosphate buffer solution (PBS), cell culture plate, cell culture dish were purchased from the American company C. Lipofectamine was purchased from the American company I. PVDF membrane was purchased from the American company M. Protein Marker and ECL luminescence reagent were purchased from the American company T. Tween-20, sodium chloride, chloroform, methanol, isopropyl alcohol, anhydrous ethanol, glacial acetic acid, glycerol, and disodium phosphate, Potassium chloride was purchased from a chemical company, phenyl methyl sul fonyl fluoride (PMSF), protein sampling buffer (5x), 35% gel, protein quantification BCA kit, protein lysate RIPA, phosphatase inhibitor was purchased from a biotechnology company.

Sealing membrane was purchased from P Company (USA), lipopolysaccharide (LPS), tetramethyl ethylene diamine (TEMED), transforming growth factor β1 (TGF-β1) were purchased from S Company (USA), and methacrylamide, glycine,

Tris, acrylamide, and sodium dodecyl sulphate (SDS) were purchased from a biotechnology company.

3.2.2. Wild baicalin preparation

Wild baicalin is almost insoluble in any solvent under acidic conditions, so it is difficult to acid hydrolyse it to wild baicalin. In this paper, based on the existing related literature, the preparation method of SCU was improved as follows:

Wild baicalin (2.5 g, 5.33 mmol) was added into a 250 ml single-necked round-bottomed flask, and dissolved with 50 ml of 95% ethanol, then 20 ml of concentrated sulphuric acid was added dropwise into the reaction flask, and while dropping and adding, the reaction solution was uniformly stirred with a magnetic brick, and after completion, the reaction solution was heated to increase the temperature to 90 °C, and the reaction was carried out for 5 h. During this time, the reaction was detected by TLC (Thin-layer chromatography), and when the reaction was complete, the When the reaction was complete, the reaction bottle was immediately poured into the reaction liquid volume of 2.5 times the pure water, filtered through the solid, washed with water to neutral, vacuum dried. The dried solid was dissolved in methanol, to which appropriate amount of glacial acetic acid was added, and recrystallised under nitrogen protection in a dry, light-proof and cool place. The crystalline product was filtered and drained to obtain 1.46 g of yellow solid of the target product with 58.4% yield.

3.2.3. SCU/DOX drug preparation

In this experiment, three different loading methods were tried to load the drugs and the three loading methods were compared. Preparation of SCU/DOX nanoparticles. The SCU and DOX drugs were loaded simultaneously into the inner cavity of ferritin by heat treatment method Detailed procedure is as follows:

(1) SCU and DOX were dissolved in PBS and ethanol solutions, respectively.

(2) SCU and DOX drugs were added to Tris-HCl (22 mM, pH = 8.1) solution at a ferritin concentration of 0.75 mg/mL.The molar ratio of UA to HFtn was 420:1, and optimisation experiments were performed for different input ratios of SCU and DOX (2:8, 1:9, 1:4, 3:7 and 2:3). It is worth noting that the SCU drug addiction process needs to be dripped slowly and magnetic stirring is required during the dripping process to prevent local ethanol concentration from too high protein denaturation.

(3) The protein-drug mixture was incubated at 55°C for 5h in a thermostatic water bath.

(4) The mixture at the end of incubation was centrifuged at 11,000 rpm for 20 min.

(5) The supernatant was taken and dialysed in PBS for 24 h to remove the free drug.

(6) The dialysed liquid was centrifuged at 5500 g for 6 min, and the resulting supernatant was passed through a 0.55 μm aqueous membrane to obtain SCU/DOX nanodrugs.

(7) The control group used in this experiment, HF-DOX and HF-SCU were prepared in the same way as the method of co-loading two drugs.

(8) The control group of this experimental method also involves a low

concentration of urea loading/DOX with ferritin present in GFC solution at pH 7.1 and a urea concentration of 22 mM. The mixture was incubated for 2.5 h at 5 ℃, then SCU drug was added with slow stirring for 30 min, followed by dialysis in PBS for 30 h. After dialysis, the protein liquid from the dialysate bag of the above steps was centrifuged for 6 min and filtered to obtain Urea-HF-SCU loaded by urea method.

(9) The content of DOX encapsulated was detected by enzyme marker, and the content of SCU encapsulated was determined by liquid chromatography.

(10) The loading capacity (LC) and encapsulation efficiency (EE) of DOX or SCU were calculated as:

$$LC = \text{Packet quality/Iron protein*100\%} \tag{8}$$

$$EE = \text{Packet quality/Input drug quality*100\%} \tag{9}$$

3.3. Experimental methodology

3.3.1. SCU/DOX drug analysis methods

(1) Establishment of standard curve

Using an analytical balance, 1.2 mg of SCU/DOX was weighed and added into a 6.0 mL brown volumetric flask, and then dissolved in an appropriate amount of ultrapure water and fixed, to formulate a SCU/DOX solution with a concentration of 250 μg/mL. Take an appropriate amount of the prepared SCU/DOX solution and add an equal amount of ultrapure water to dilute it sequentially to obtain 180 μg/mL, 120 μg/mL, 60 μg/mL, 6 μg/mL, 3 μg/mL, 1 μg/mL gradient diluted SCU/DOX solution. Take 120 μL of each group of gradient dilution solutions were added to the high-performance liquid chromatography spiking tube, the chromatographic peaks of each group of SCU/DOX solution were measured, and the peak area was obtained by integrating, the standard curve of SCU/DOX concentration was plotted, with the horizontal coordinate as the concentration and the vertical coordinate as the peak area, and the R^2 of the standard curve was calculated, in which, the high-performance liquid chromatography column was Agilent Eclipse XBD-C, and the detection temperature was 32 ℃, and the detection temperature was 0.01 ℃, and the detection temperature was 0.01 ℃, and the detection temperature was 0.01 ℃, and the detection temperature was 0.01 ℃. The column temperature condition was 32 ℃, the detection characteristic wavelength was 255 nm, the single injection volume was 25 μL, and the mobile phase aqueous solution was prepared as sodium dodecyl sulphate (SDS) 2.91 g, 1.35 mL of H3PO4, and 1100 mL volumetric flasks of ultrapure water were fixed.

(2) Proprietary experiments

In order to investigate whether different substances in SCU and ethanol solvent and SCU would affect the detection of SCU/DOX by HPLC, the above chromatographic conditions were used for detection, combined with different experimental samples. The peak times and chromatogram peak shapes of different samples were compared to examine whether the solvents and SCU/DOX standard samples affect the detection of SCU/DOX, and whether the peaks of each group were completely separated.

(3) Stability

Weigh 5.5 mg of SCU/DOX using an analytical balance, carefully add it into a 55 mL brown volumetric flask, add appropriate amount of ultrapure water to dissolve and settle the volume, prepare a 120 μg/mL SCU/DOX solution, and leave it at room temperature. The SCU/DOX standard solution was sampled every two hours starting from 0.5 h. The time points were 2.5 h, 4.5 h, 6.5 h, 8.5 h, 10.5 h, and 12.5 h. The SCU/DOX content of each sample was detected by HPLC assay for five times.

3.3.2. Cell proliferation and toxicity effects

In order to clarify the effects of SCU/DOX nanodrugs on cellular value-adding and toxicity inhibition, this paper designed a method to measure the effects of SCU/DOX drugs on cell proliferation and toxicity at different pH. The specific steps are as follows:

(1) Dilute concentrated hydrochloric acid to 1.5 mol/L dilute hydrochloric acid with sterile ultrapure water.

(2) Dilute hydrochloric acid was added dropwise to DMEM high sugar medium containing 12% FBS using a rubber-tipped burette and mixed thoroughly.

(3) Determine the pH of the medium using a pH meter and adjust the medium pH to 7.0.

(4) The cells in the petri dishes were digested, centrifuged and resuspended using complete medium, then counted using a cell counter, and the cell concentration was adjusted to 5×10^5 cells/mL.

(5) Inoculate the cells into 108-well plates at an inoculum of 6000 cells per well, and place them in a cell culture incubator at 36 ℃ for overnight adherence culture.

(6) Discard the cell culture supernatant, mix the concentration of the drug to be measured with the medium at pH 7.5 or 6.8 and adjust to the concentration required for the experiment, and add 110 μL per well to the 108-well plate.

(7) After continuing to incubate the cells for 20 h, add 12 μL CCK-8 solution per well under the condition of avoiding light, gently tap the 108-well plate, mix well, and place it in the cell culture incubator to incubate for 1 h–2 h.

(8) Determine the absorbance of the solution at 500 nm using a multifunctional enzyme marker and collect the data.

3.3.3. SCU/DOX drug release testing

HPLC was used to test the release experiment of SCU/DOX nanodrugs. Firstly, HPLC standard curve of SCU/DOX nanodrugs was made. The SCU/DOX nanomedicine solutions with concentration gradients of 0.3 μg/mL, 0.6 μg/mL, 1.2 μg/mL, 1.8 μg/mL, 3.6 μg/mL, 7.2 μg/mL and 14.4 μg/mL were prepared, and the samples were prepared with PBS buffer solution of pH 7.2 in the ratio of 150 μL:50 μL. The prepared solution was filtered and then loaded into a 2.5 mL special test vial for HPLC, and HPLC tests were performed for each concentration of the solution in turn.

PCHP nanoparticles (1.5 mg/mL) were added to five dialysis bags with a molecular weight cut-off of 1000 Da, each 0.8 mL. The sealed dialysis bags were placed into the bottom of a 60 mL centrifuge tube, to which 6 mL of pure PBS (pH = 7.2), 6 mL of 1.5 mM, and 15 mM hydrogen peroxide solution were added,

respectively. At regular intervals (1 h, 5 h, 10 h, 15 h, 20 h, 25 h, 30 h, 35 h, 40 h, 45 h) the 6 mL of buffered release solution in the centrifuge tubes was removed and new release solution was added. The released solution was mixed with methanol in the ratio of 1:4 and the samples were prepared, and the content of SCU/DOX nanomedicine was detected by HPLC, and finally the release curves of SCU/DOX nanomedicine were plotted under different conditions.

4. Experimental results

Biomimetic nanoparticles can enhance antibiotic penetration and remove bacteria from biofilms through interactions with complex biofilm matrices. They also act on bacterial cells through electrostatic adsorption, van der Waals forces, receptor-ligand binding, etc., increasing uptake by mechanisms such as endocytosis and megalocytosis mediated by lattice proteins or follicular proteins/lipid rafts, and aggregating along the metabolic pathway after crossing the bacterial cell membrane. The slow and controlled release of nanocarriers and targeted drug delivery can control the release of the drug, increase plasma antibiotic levels and reduce toxic side effects. This chapter focuses on the data analysis of drug-carrying performance and targeted therapeutic ability of biomimetic nanoparticles for delivering release of wild baicalin and adriamycin, which provides a reference for improving the drug-carrying performance and targeted therapeutic ability of nanoparticles.

4.1. SCU/DOX drug properties

4.1.1. Cell viability inhibition

For the effect of SCU/DOX nanomedicine on the viability of mouse cells, this paper used the MTS method to study the inhibitory effect of SCU/DOX nanomedicine on mouse cells after 20 h and 40 h of action at different concentrations. **Figure 3** shows the results of the effect of SCU/DOX nanomedicine on the viability of mouse cells, where **Figure 3a,b** shows the results of the action for 20 h and 40 h, respectively, and #, ###, #### represent $P < 0.1$, $P < 0.05$ and $P < 0.01$, respectively.

After 20h of action on mouse cells using SCU/DOX nanomedicine, when the concentration of SCU/DOX nanomedicine was elevated from 10 μM to 16,010 μM, the viability of mouse cells was reduced from 82.54% to about 47.69%. After 40h of action, mouse cell viability decreased from 82.54% to 31.47%. It can be seen that the inhibitory effect of SCU/DOX nanomedicine on mouse cell viability was more and more obvious as the concentration of SCU/DOX nanomedicine administered was elevated.

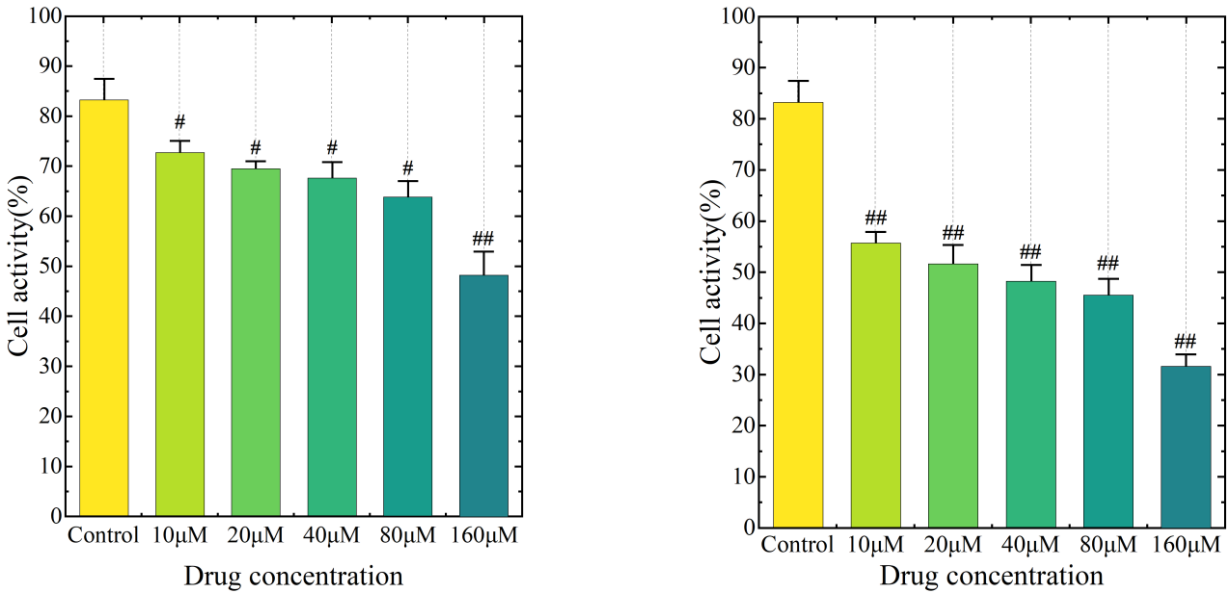

Figure 3. Effects of cell activity **(a)** SCU/DOX-20h; **(b)** SCU/DOX-40h.

4.1.2. Inhibition of cell proliferation

After verifying the inhibitory effect of SCU/DOX nanoparticles on the viability of mouse cells, in order to further verify the effect of SCU/DOX nanodrug particles on cell proliferation, the effect of SCU/DOX on the proliferative effect of mouse cells was detected by MTT method. According to the inhibition of SCU/DOX nanomedicine on mouse cell viability, 10 μM and 20 μM were selected as the combined concentrations for testing in this paper. The inhibitory effects of SCU/DOX nanomedicine on mouse cell proliferation are shown in **Figure 4**, in which **Figure 4a** to **Figrue 4d** show the results of SCU alone, DOX alone, SCU/DOX (10 μM) and SCU/DOX (20 μM) experimental results.

The results showed that the combination of 10 μM and 20 μM with different concentrations of SCU/DOX produced different degrees of synergistic effects, and the inhibitory effect of SCU/DOX nanomedicine on the proliferation of mouse cells was significantly enhanced. The IC_{50} value of SCU/DOX on mouse cells was calculated, which was 59.42 μM when used alone, and decreased to 11.57 μM and 8.75 μM when combined with 10 μM and 20 μM, respectively, and the reversal of the resistance multiplicity was 5.14-fold and 6.79-fold, respectively. After statistically obtaining the IC_{50} values of SCU/DOX nanodrugs on mouse cells, the Q value of each combined concentration was calculated using the golden formula to determine whether the drugs had a synergistic effect when combined at that concentration. SCU and DOX were considered to be synergistic when the Q value was greater than 1.2. It was calculated that in mouse cells, SCU/DOX had synergistic effects under the conditions of co-administration at each concentration.

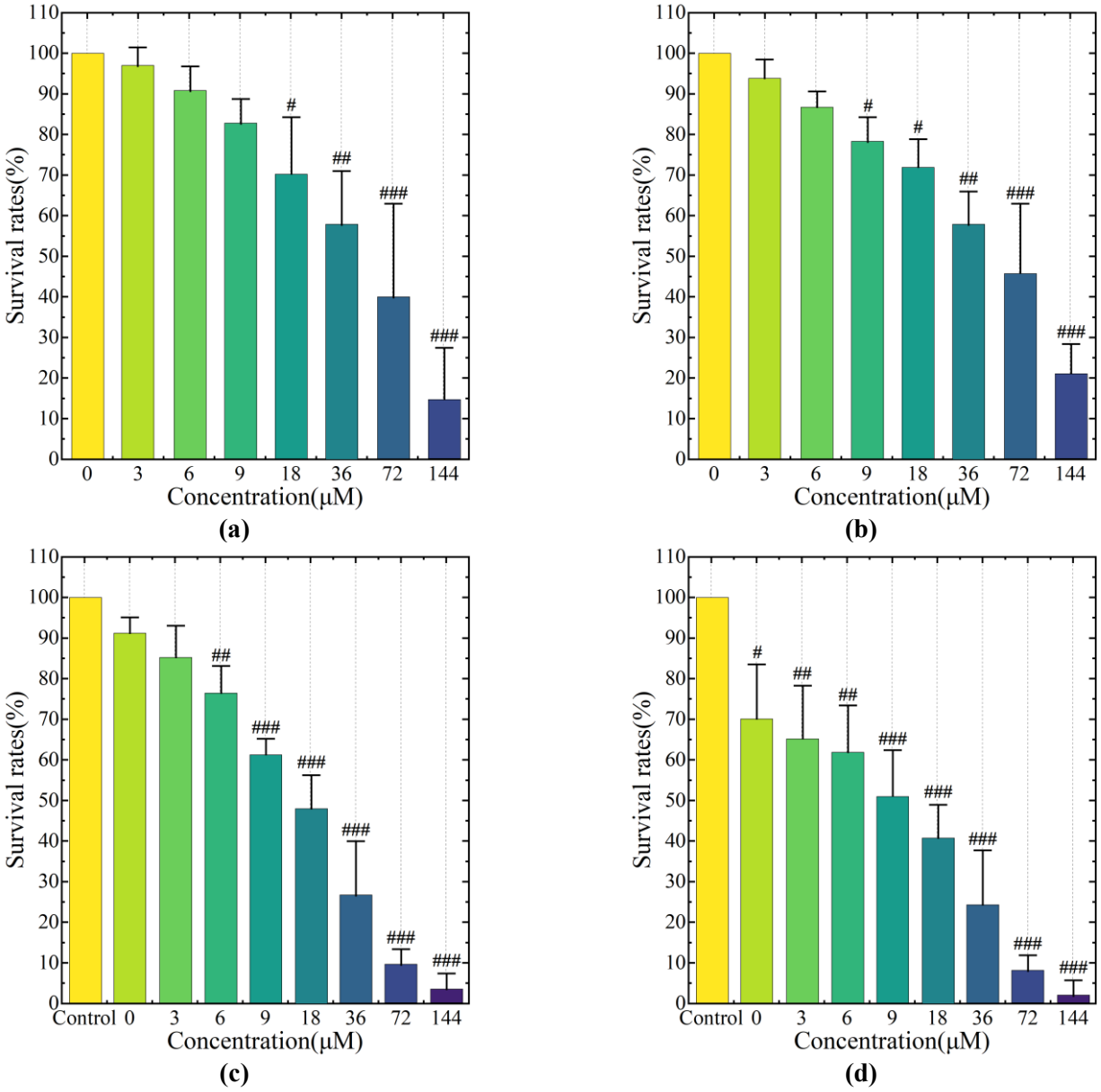

Figure 4. Inhibition of cell proliferation **(a)** SCU; **(b)** DOX; **(c)** SCU/DOX (10 μM); **(d)** SCU/DOX (20 μM).

4.1.3. Synergistic anti-tumour effects

In order to verify the inhibitory effect of SCU/DOX nanomedicine prepared in this paper on mouse tumour cells and to better explain the drug-carrying properties of the drug, the in vivo anti-tumour effect of SCU/DOX nanomedicine was further analysed in this paper by constructing an animal model of hepatocellular carcinoma. Each mouse was inoculated with 2×10^5 H20 mouse hepatocellular carcinoma cells, and when the tumour volume was 120 mm^3, the mice were divided into four groups of Control, SCU, DOX and SCU/DOX. Tumour volume and tumour weight of the mice were recorded on every other day for 16 days to assess the drug-carrying properties of SCU/DOX nanoparticles, which was also used to evaluate the effectiveness of SCU/DOX nanomedicines. **Figure 5** shows the synergistic anti-tumour effect of SCU/DOX nanomedicines, where **Figures 5a–c** show the results of tumour weight, tumour volume and body weight changes in mice, respectively.

The results showed that compared with the control group, after 16 days of administration, the mouse tumour volume was reduced from 15.1 × 10^2 mm^3 in the control group to 6.05 × 10^2 mm^3 in the SCU/DOX group, and the weight of the tumour was reduced from the original 1.45 g to 0.52 g, and there was also a significant change in the body weight of the mice. Compared with the control group, the application of SCU/DOX nanoparticles was able to inhibit the tumour growth of mice more significantly, despite the inhibitory effect of SCU and DOX administered alone. This also shows to some extent that SCU/DOX nanoparticles have better drug-carrying properties, which can effectively transport wild baicalin and adriamycin into the cells and achieve effective treatment of tumour cells.

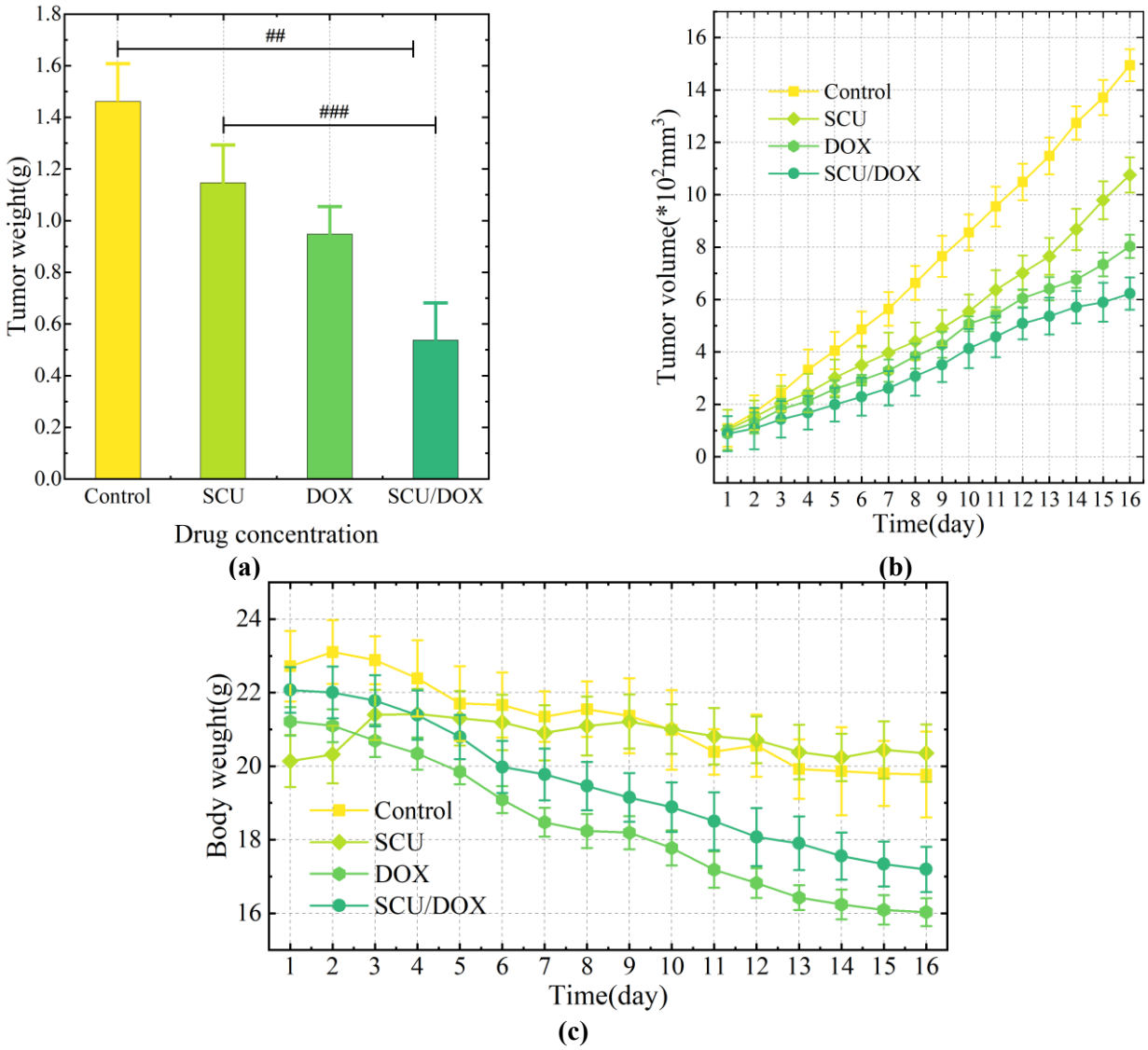

Figure 5. Synergistic anti-tumor effect **(a)** tumor weight; **(b)** tumor volume; (c) weight change results.

4.2. SCU/DOX drug release

4.2.1. SCU/DOX drug release performance

(1) Esterase response controls drug release

To investigate the esterase responsiveness of SCU/DOX nanodrug particles, high performance liquid chromatography was used to test the in vitro drug release

performance of SCU/DOX nanodrug particles at pH 7.2 + 50 units/mL esterase conditions, and the release results are shown in **Figure 6**. The drug release rate of SCU was accelerated by the addition of esterase, and the cumulative drug release was 16.95% at 2 h and 24.69% at 20 h, which was about 2.75 times higher than that of the esterase-free condition (8.97%), indicating that the esterase had a facilitating effect on the release of SCU. Similarly, the cumulative drug release of SCU/DOX at 2h was 11.18% and at 20h was 37.55% higher than that of the esterase-free condition (17.61%). However, the effect of esterase on drug release was less compared to pH, which may be due to the fact that the core cross-linking resulted in the structural stabilisation of SCU/DOX, the ester bonds on the polymer were slow to break, and the drug was released into the external medium mainly by diffusion.

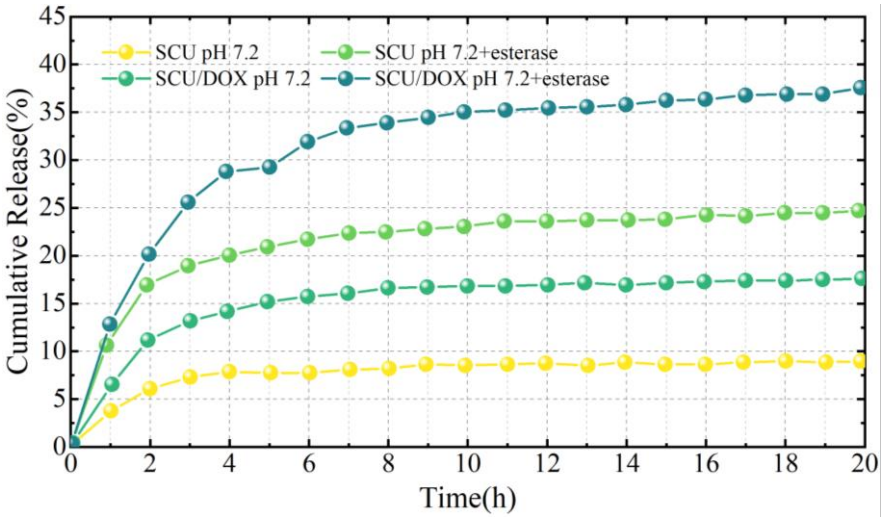

Figure 6. Vitro release curve.

(2) pH response to control drug release

SCU/DOX nanodrug particles are constructed to reduce drug leakage in the blood circulation and to achieve sustained and accurate release within the tumour cells, and should therefore be stable in a simulated normal physiological environment and rapidly release the drug in a simulated tumour lysosomal environment. Since the release of anticancer drugs from within to external media is accompanied by changes in drug concentration, the in vitro drug release behaviour of SCU/DOX nanodrug particles under different conditions (pH 7.2 and pH 5.5) was investigated using high performance liquid chromatography (HPLC) in order to evaluate the effect of different pH on the release of the drug, and the results of the release are shown in **Figure 7**.

Under normal physiological environment (e.g., blood) pH 7.2, SCU released the drug more slowly, with only 8.19% released in the first 10 h. The cumulative release of the drug in 90 h was still low at 10.19%. In contrast, using pH 5.5 acetate buffer to simulate the tumour microenvironment, the cumulative drug release from SCU reached 20.14% in 5 h, 52.73% in 10 h, which was a significantly accelerated release rate, and then the drug release tended to plateau, with a cumulative release of 59.59% in 90 h (low), which was probably due to the fact that acylated stilbene bonding only occurred under pH 5.5, and only partial bond breaking occurred. For

SCU/DOX, drug release was faster than that of SCU both at pH 7.2 and 5.5, which was attributed to the fact that the imine bond was more susceptible to breakage than the acylhydrazone bond. The cumulative drug release was 15.73% at pH 7.2 for 10 h and 18.61% for 90 h. At pH 5.5, the rate of drug release was significantly higher, reaching 59.78% at 5 h, 77.98% cumulative drug release at 10h, and 80.18% at 90h, which was about 4.31 times higher than that under pH 7.2. It indicates that different concentrations can indeed enhance the stability of SCU/DOX drug nanoparticles, which can effectively inhibit drug release and prevent drug leakage. And when the drug-carrying nanoparticles reach the tumour cells or tissues, the weak acidic environment in the cell will destroy the structure of the nanoparticles, the cross-linking bond will be broken, and the SCU/DOX nanoparticles will be rapidly de-cross-linking, and the barrier that hinders the drug diffusion disappeared, so as to achieve the rapid and large amount of drug release, which has a good pH-stimulated response release performance.

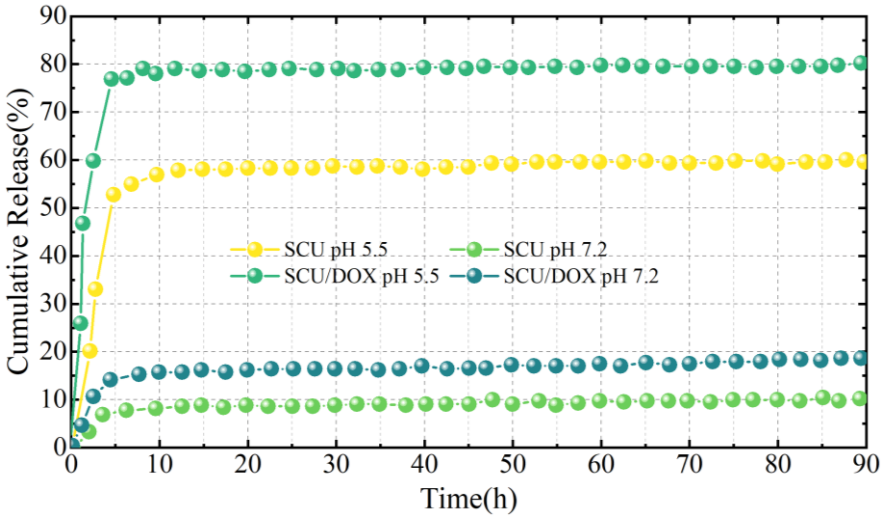

Figure 7. pH response control drug release.

4.2.2. SCU/DOX drug release kinetics

For SCU/DOX nanoparticles drug release profiles, combined with the models related to drug release kinetics given in the previous section, the SCU/DOX nanoparticles at different pH were fitted by the zero-order, one-order, Higuchi, Korsmeyer-Peppas, Hixon-Crowell, and Baker-Lonsdale models, respectively. drug release was fitted and the results are shown in **Figure 8**. Where **Figures 8a–f** show the fitting results of each model, respectively.

From the figure, it can be seen that the best fits were obtained using the Higuchi model and the Baker-Lonsdale model when the pH of the physiological environment was 7.2 and 8.1, whereas the best fits were obtained using the Korsmeyer-Peppas model for the drug release from SCU/DOX nanoparticles when the pH was 5.5 and 6.3. In general, drug release from polymer matrices can occur through two mechanisms, namely, diffusive release and solubilisation release by matrix degradation. pH values of 7.2 and 8.1 showed good fit using the Higuchi model, which implies that drug release from SCU/DOX nanoparticles exhibits typical Fickian diffusion. The Baker-Lonsdale model is an evolution from the Higuchi

model, which evolved from the Baker-Lonsdale model and is suitable for the simulation of drug release from spherical matrices. pH values of 7.2 and 8.1 showed a good fit of the release process using the Baker-Lonsdale model, which further confirms that at this time the release of SCU/DOX nanoparticles from the cells is dominated by diffusion. pH values of 5.5 and 6.3 showed a good fit of the Korsmeyer- Peppas model provided a better fit for SCU/DOX nanoparticle drug release and the characteristic indices were in the range of 0.428 to 0.847, showing an anomalous or non-Fickian diffusion process. This result suggests that the drug release mechanism of SCU/DOX nanoparticle drugs at pH 5.5 and 6.3 is a co-existence of diffusion and structural relaxation/solubilisation.

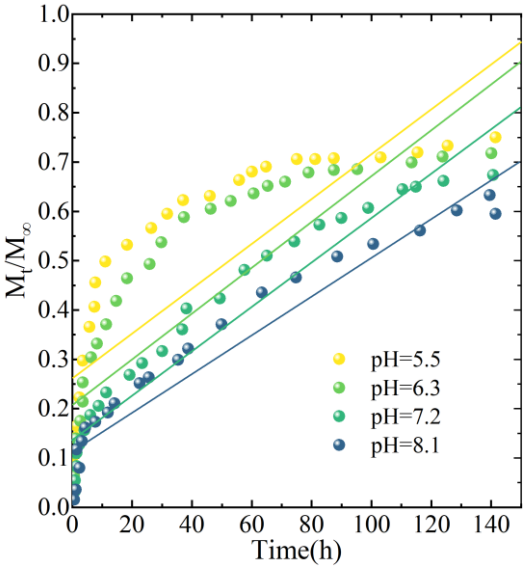

(a)

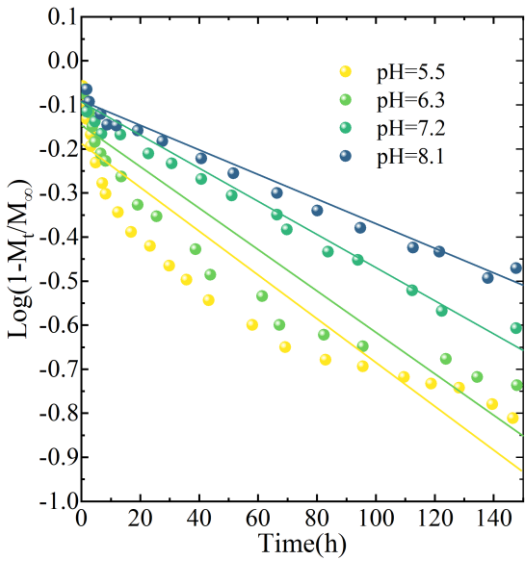

(b)

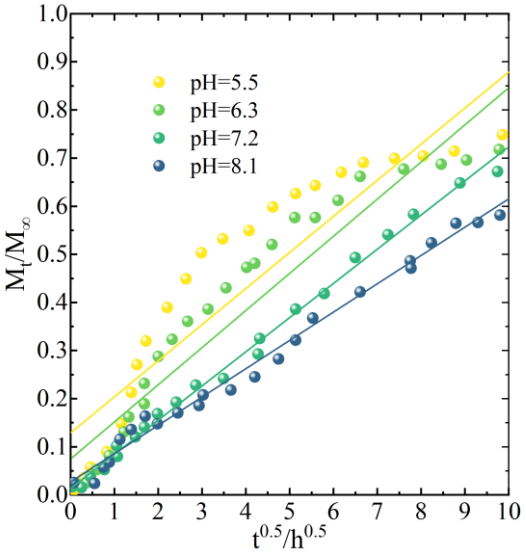

(c)

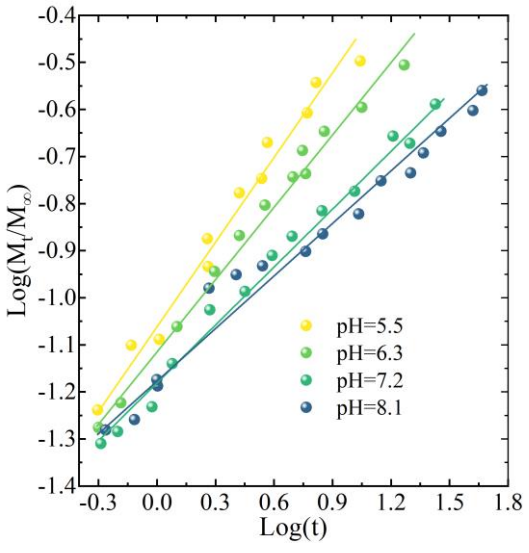

(d)

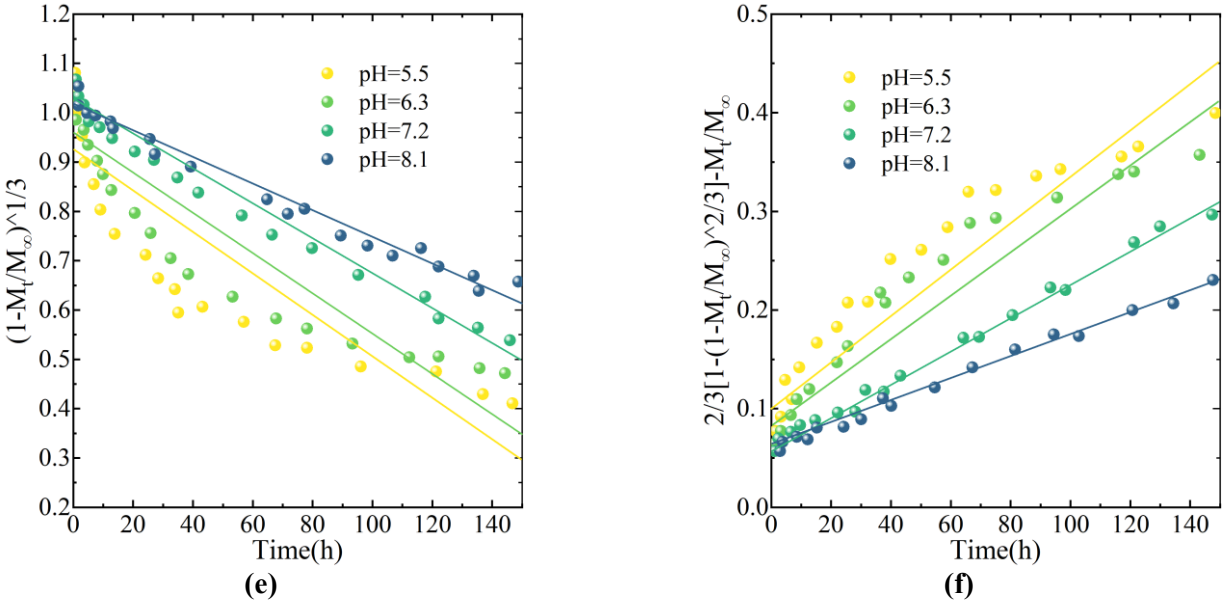

Figure 8. The drug releases the dynamic curve **(a)** zero stage; **(b)** first stage; **(c)** Higuchi; **(d)** Korsmeyer-Peppas; **(e)** Hixon-Crowell; **(f)** Baker-Lonsdale.

5. Conclusion

Biomimetic nanoparticle preparation of wild baicalein and adriamycin using a nanodrug delivery system helps to enhance drug loading and targeted therapeutic effects. After the preparation of SCU/DOX nanoparticles, their specific drug properties and kinetic performance were analysed by data.

(1) When the concentration of SCU/DOX nanomedicine was elevated from 10 μM to 16010 μM, the mouse cell viability was reduced from 82.54% to about 47.69%. With the deepening of the concentration of SCU/DOX nanomedicine, the inhibitory effect on the activity of tumour cells became more and more obvious.

(2) In the inhibitory effect on the proliferation of tumour cells, the IC_{50} value of SCU drug alone was 59.42 μM, and after the use of SCU/DOX nanoparticles, its IC_{50} value decreased to 8.75 μM at the lowest level, and the reversal of the resistance multiplier was 6.79 times. Combining SCU with DOX can effectively enhance the inhibition of tumour cell proliferation.

(3) After 16 days of SCU/DOX nanoparticles administration, the tumour volume of mice decreased from 15.1 × $10^2$$mm^3$ to 6.05 × $10^2$$mm^3$, the tumour weight decreased by 64.14%, and there was a large change in the body weight of the mice.SCU/DOX nanoparticles have better drug-carrying properties, and they can transport wild baicalin and adriamycin into the cells efficiently to achieve the effective treatment.

(4) The cumulative drug release of SCU/DOX nanoparticles was 11.18% at 2 h, and the cumulative drug release after 20 h was higher than that in the esterase-free condition (17.61%). The drug release kinetics of SCU/DOX nanoparticles differed at different pH values, and the diffusion effects were also different for the targeting of tumour cells.

Author contributions: Conceptualization, MW and YL; methodology, SZ; software, SZ; validation, MW, YL and SZ; formal analysis, MW; investigation, YL; resources, YL; data curation, MW; writing—original draft preparation, MW; writing—review and editing, SZ; visualization, YL; supervision, MW; project administration, MW; funding acquisition, YL. All authors have read and agreed to the published version of the manuscript.

Funding: This work was supported by 2024 Henan Province Science and Technology Key Project (242102310572) and Key Research Project Plan for Higher Education Institutions in Henan Province (24B320008).

Ethical approval: Not applicable.

Conflict of interest: The authors declare no conflict of interest.

References

1. Mazari, S. A., Ali, E., Abro, R., Khan, F. S. A., Ahmed, I., Ahmed, M., ... & Shah, A. (2021). Nanomaterials: Applications, waste-handling, environmental toxicities, and future challenges–A review. Journal of Environmental Chemical Engineering, 9(2), 105028.
2. Das, S., Sen, B., & Debnath, N. (2015). Recent trends in nanomaterials applications in environmental monitoring and remediation. Environmental Science and Pollution Research, 22, 18333-18344.
3. Bissessur, R. (2020). Nanomaterials applications. In Polymer science and nanotechnology (pp. 435-453). Elsevier.
4. Gajanan, K., & Tijare, S. N. (2018). Applications of nanomaterials. Materials Today: Proceedings, 5(1), 1093-1096.
5. Kshersagar, J., Bohara, R. A., & Joshi, M. G. (2019). Pharmacological study of hybrid nanostructures. In Hybrid Nanostructures for Cancer Theranostics (pp. 87-104). Elsevier.
6. Sarma, A., Bania, R., Devi, J. R., & Deka, S. (2021). Therapeutic nanostructures and nanotoxicity. Journal of Applied Toxicology, 41(10), 1494-1517.
7. Nikezić, A. V. V., Bondžić, A. M., & Vasić, V. M. (2020). Drug delivery systems based on nanoparticles and related nanostructures. European Journal of Pharmaceutical Sciences, 151, 105412.
8. Talapin, D. V., & Shevchenko, E. V. (2016). Introduction: nanoparticle chemistry. Chemical Reviews, 116(18), 10343-10345.
9. Modena, M. M., Rühle, B., Burg, T. P., & Wuttke, S. (2019). Nanoparticle characterization: what to measure?. Advanced Materials, 31(32), 1901556.
10. Titus, D., Samuel, E. J. J., & Roopan, S. M. (2019). Nanoparticle characterization techniques. In Green synthesis, characterization and applications of nanoparticles (pp. 303-319). Elsevier.
11. Ciucă, A. G., Grecu, C. I., Rotărescu, P., Gheorghe, I., Bolocan, A., Grumezescu, A. M., ... & Andronescu, E. (2017). Nanostructures for drug delivery: pharmacokinetic and toxicological aspects. In Nanostructures for Drug Delivery (pp. 941-957). Elsevier.
12. Pawar, V., Maske, P., Khan, A., Ghosh, A., Keshari, R., Bhatt, M., & Srivastava, R. (2023). Responsive nanostructure for targeted drug delivery. Journal of Nanotheranostics, 4(1), 55-85.
13. Xu, X., Ho, W., Zhang, X., Bertrand, N., & Farokhzad, O. (2015). Cancer nanomedicine: from targeted delivery to combination therapy. Trends in molecular medicine, 21(4), 223-232.
14. Nimesh, S., Chandra, R., & Gupta, N. (2017). Advances in nanomedicine for the delivery of therapeutic nucleic acids. Woodhead Publishing.
15. Jahangirian, H., Lemraski, E. G., Webster, T. J., Rafiee-Moghaddam, R., & Abdollahi, Y. (2017). A review of drug delivery systems based on nanotechnology and green chemistry: green nanomedicine. International journal of nanomedicine, 2957-2978.
16. Uchida, S., Perche, F., Pichon, C., & Cabral, H. (2020). Nanomedicine-based approaches for mRNA delivery. Molecular pharmaceutics, 17(10), 3654-3684.
17. Lynch, I., & Dawson, K. A. (2020). Protein–nanoparticle interactions. Nano-enabled medical applications, 231-250.

18. Zhang, B., Hu, Y., & Pang, Z. (2017). Modulating the tumor microenvironment to enhance tumor nanomedicine delivery. Frontiers in pharmaco.
19. Tianyao Wang,Yaochen Cao,Jinsheng Xiong & Liru Li. (2025). Construction of a nano-fluorescent polymer drug delivery system for breast cancer treatment. Journal of Molecular Structure(P1),139820-139820.
20. Munerah Alfadhel. (2024). Nanofiber-Based Drug Delivery Systems: A Review on Its Applications, Challenges, and Envisioning Future Perspectives. Current drug delivery.
21. Shayeri Chatterjee Ganguly,Beduin Mahanti,Soumya Ganguly & Subhabrota Majumdar. (2024). Bovine serum albumin as a nanocarrier for efficient encapsulation of hydrophobic garcinol-A strategy for modifying the in vitro drug release kinetics. International journal of biological macromolecules(P1),134651.
22. Lu Yang, Xianfeng Liu, Siyin Chen, Jiayi Sun, Yiwen Tao, Liyuan Ma... & Xianli Meng. (2024). Scutellarin ameliorates mitochondrial dysfunction and apoptosis in OGD/R-insulted HT22 cells through mitophagy induction. Biomedicine & pharmacotherapy = Biomedecine & pharmacotherapie117340.